Eukaryotic Cell

Contribution of Galactofuranose to the Virulence of the Opportunistic Pathogen *Aspergillus fumigatus*

Philipp S. Schmalhorst, Sven Krappmann, Wouter Vervecken, Manfred Rohde, Meike Müller, Gerhard H. Braus, Roland Contreras, Armin Braun, Hans Bakker and Françoise H. Routier

Eukaryotic Cell **2008, 7(8):1268. DOI: 10.1128/EC.00109-08. Published Ahead of Print 13 June 2008.**

EUKARYOTIC CELL, Aug. 2008, p. 1268–1277 Vol. 7, No. 8
1535-9778/08/$08.00+0 doi:10.1128/EC.00109-08

Contribution of Galactofuranose to the Virulence of the Opportunistic Pathogen *Aspergillus fumigatus*▽

Philipp S. Schmalhorst,[1] Sven Krappmann,[2]† Wouter Vervecken,[3] Manfred Rohde,[4] Meike Müller,[5] Gerhard H. Braus,[2] Roland Contreras,[3] Armin Braun,[5] Hans Bakker,[1] and Françoise H. Routier[1]*

Department of Cellular Chemistry, Hannover Medical School, Hannover, Germany[1]; Department of Molecular Microbiology and Genetics, Georg August University, Göttingen, Germany[2]; Department of Molecular Biology, Ghent University, and Department for Molecular Biomedical Research, VIB, Ghent, Belgium[3]; Department of Microbial Pathogenicity, Helmholtz Centre for Infection Research, Braunschweig, Germany[4]; and Department of Immunology, Allergology and Immunotoxicology, Fraunhofer Institute of Toxicology and Experimental Medicine, Hannover, Germany[5]

Received 27 March 2008/Accepted 9 June 2008

The filamentous fungus *Aspergillus fumigatus* is responsible for a lethal disease called invasive aspergillosis that affects immunocompromised patients. This disease, like other human fungal diseases, is generally treated by compounds targeting the primary fungal cell membrane sterol. Recently, glucan synthesis inhibitors were added to the limited antifungal arsenal and encouraged the search for novel targets in cell wall biosynthesis. Although galactomannan is a major component of the *A. fumigatus* cell wall and extracellular matrix, the biosynthesis and role of galactomannan are currently unknown. By a targeted gene deletion approach, we demonstrate that UDP-galactopyranose mutase, a key enzyme of galactofuranose metabolism, controls the biosynthesis of galactomannan and galactofuranose containing glycoconjugates. The *glfA* deletion mutant generated in this study is devoid of galactofuranose and displays attenuated virulence in a low-dose mouse model of invasive aspergillosis that likely reflects the impaired growth of the mutant at mammalian body temperature. Furthermore, the absence of galactofuranose results in a thinner cell wall that correlates with an increased susceptibility to several antifungal agents. The UDP-galactopyranose mutase thus appears to be an appealing adjunct therapeutic target in combination with other drugs against *A. fumigatus*. Its absence from mammalian cells indeed offers a considerable advantage to achieve therapeutic selectivity.

The filamentous fungus *Aspergillus fumigatus* is the primary cause of invasive aspergillosis, an often fatal condition affecting people with a weakened immune system. Along with the immunocompromised population, the incidence of invasive aspergillosis is constantly growing, but therapy remains problematic. The sterol binding polyene amphotericin B and the ergosterol biosynthesis inhibitor itraconazole have long been the drugs of choice for treatment of this infection, but because of their higher efficacy and lower toxicity, new triazoles, such as voriconazole or posaconazole, are supplanting these drugs (28, 33). Additionally, a novel class of antifungal agents called the echinocandins provides further options for treatment. These compounds inhibit the synthesis of β1,3-glucan, a major cell wall component, with resultant osmotic instability and lysis (12). Their minimal toxicity and synergistic activity with voriconazole and amphotericin B make them particularly attractive for combination therapy, although clinical validation is still awaited (33, 35). Despite these advances in therapy, invasive aspergillosis is often associated with significant morbidity and mortality, emphasizing the need for novel therapeutic strategies based on the fundamental knowledge of *A. fumigatus* pathogenesis.

The development of echinocandins illustrates the viability of targeting enzymes involved in cell wall biosynthesis and encourages the development of chitin synthesis inhibitors. Like glucan and chitin, galactomannan is an abundant component of the *A. fumigatus* cell wall (4). This polysaccharide, composed of a linear mannan core branched with short β1,5-linked galactofuranose (Gal*f*) chains (22), is bound covalently to the cell wall β1,3-glucan, anchored to the lipid membrane by a glycosylphosphatidylinositol, or released in the environment during tissue invasion or growth in culture (3, 9, 14). Besides being an abundant component of the extracellular matrix, secreted galactomannans are used for serological diagnostic of invasive aspergillosis (1). The monosaccharide Gal*f* has also been found in the N- and O-glycans of some glycoproteins as well as the glycosphingolipids of *A. fumigatus* (23, 29, 41, 47) and thus represents an important constituent of the cell wall of this fungus. Gal*f* is otherwise infrequent in natural compounds but prevalent in pathogens. Moreover, since Gal*f* is absent from higher eukaryotes and involved in the survival or virulence of various bacteria, the enzymes involved in the biosynthesis of Gal*f* are considered attractive drug targets (32, 34).

Our understanding of Gal*f* metabolism in eukaryotes is limited. Gal*f* is most likely incorporated into cell surface components by specific galactofuranosyltransferases that use UDP-Gal*f* as a donor. The work of Trejo and colleagues in the early 1970s already suggested the existence of an enzyme converting UDP-galactopyranose into UDP-galactofuranose involved in

* Corresponding author. Mailing address: Department of Cellular Chemistry (OE 4330), Hannover Medical School, 30625 Hannover, Germany. Phone: 49 (511) 532-9807. Fax: 49 (511) 532-3956. E-mail: Routier.Francoise@mh-hannover.de.

† Present address: Research Center for Infectious Diseases, Würzburg, Germany.

▽ Published ahead of print on 13 June 2008.

TABLE 1. DNA oligonucleotides used in this study

Oligonucleotide	Sequence (5′→3′)[a]	Description (restriction site)
PS1	ATAAGCGGCCGCAAGCTGGGAACGCGATTCAA	5′ Flanking region pΔglfA reverse (NotI)
PS12	TATACCGCGGCTGCCAAGCTATCAGTTTCC	5′ Flanking region pΔglfA sense (SacII)
PS3	ATCCGGTGCTCAGGTATTCGCCA	3′ Flanking region pΔglfA sense (EcoRV)
PS4	ATCCATCGATCATATCCTATGCGGTCTCAG	3′ Flanking region pΔglfA reverse (ClaI)
PS66A	TTACGCATTCCCAGCAGTTG	Southern blot probe 1 sense
PS67A	TGCGCTGTGATGAATGGTGT	Southern blot probe 1 reverse
PS68A	TCCACAATACGTCCCCTACA	Southern blot probe 2 sense
PS69A	GTATGAACCCTCTCCCAATG	Southern blot probe 2 reverse
PS20	AAGGTCGTTGCGTCAGTCCA	Southern blot probe 3 sense
PS21	TCGATGTGTCTGTCCTCC	Southern blot probe 3 reverse
PS23s	ATGCCGCTCTCGAGGCTCGT	Site-directed mutagenesis *glfA** sense (XhoI)
PS23r	CACGAGCCTCGAGAGCGGCA	Site-directed mutagenesis *glfA** reverse (XhoI)
PS28	ATATGCGGCCGCAAACAGGAGCGAAGTAGT	5′ Flanking region pglfA* sense (NotI)
PS31	ATATCCCGGGAGTTTGGTGCTGTGGTAGGT	3′ Flanking region pglfA* reverse (XmaI)
PS78	CGTGTCTATCGTACCTTGTTGCTT	18S rRNA gene fragment sense
PS79	AACTCAGACTGCATACTTTCAGAACAG	18S rRNA gene fragment reverse
Probe	**FAM**-CCCGCCGAAGACCCCAACATG-**TAMRA**	qPCR hybridization probe

[a] Restriction sites are underlined. TAMRA, 6-carboxytetramethylrhodamine.

the biosynthesis of the fungal cell wall (48). This enzyme, named UDP-galactopyranose mutase (UGM) and encoded by the *glf* gene, was described first for bacteria (17, 30, 50) and lately for several eukaryotic pathogens, including *A. fumigatus* (2, 5). UGM is to date the only characterized enzyme involved in the biosynthesis of galactofuranose-containing molecules in eukaryotes, whereas several galactofuranosyltransferases have been described for bacteria (15, 19, 27, 51). The identification of this enzyme, highly conserved among lower eukaryotes and present in many fungi, enables studies of the biological role of galactofuranose in these organisms. The present report highlights the role of galactofuranose in *A. fumigatus* growth and virulence.

MATERIALS AND METHODS

Strains, media, and growth conditions. *A. fumigatus* clinical isolate D141 (38) was used as the wild-type (wt) strain in this study. All strains were grown at 37°C on *Aspergillus* minimal medium (AMM) containing 1% D-glucose as the carbon source and 70 mM $NaNO_3$ as the nitrogen source (36), unless otherwise stated. Phleomycin or 5-fluoro-2′-deoxyuridine (FUDR) was added at 30 μg/ml or 100 μM, respectively, for selection purposes.

Generation of *A. fumigatus* mutant strains. The 5′ and 3′ flanking regions (1.5 and 2 kb, respectively) of the *A. fumigatus glfA* coding sequence were amplified from genomic DNA by PCR with primers PS12/PS1 and PS3/PS4 (Table 1), respectively, and cloned into the pBluescript II SK(−) vector (Stratagene) by use of the restriction sites SacII/NotI and EcoRV/ClaI. A SpeI/NotI fragment released from pSK269 containing the phleo/tk blaster (18) was then inserted between the two fragments to obtain the disruption plasmid pΔglfA. For reconstitution of the *glfA* gene locus, the plasmid pglfA* was constructed as follows. The phleo/tk blaster of pΔglfA was first replaced with the original *A. fumigatus glfA* gene by homologous recombination in *Escherichia coli* strain YZ2000 (Gene Bridges, Leimen, Germany). A single point mutation was introduced by site-directed mutagenesis. Briefly, nonmethylated plasmid DNA was generated from a methylated parent plasmid by Phusion DNA polymerase (NEB) using complementary primers that both carried the desired mutation (PS23s/PS23r [Table 1]). Prior to transformation, the parental, methylated DNA strand was specifically cleaved by DpnI to selectively obtain transformants that harbored the mutated plasmid. Thus, codon 130 of the *glfA* coding sequence (GenBank accession number AJ871145) was changed from CTT to CTC, which generated a new XhoI restriction site. Since gene reconstitution by homologous recombination could not be obtained with this construct, 5′ and 3′ flanking regions were extended to 5 kb by replacement with recloned PCR fragments (primer pairs PS28/PS1 and PS3/PS31) to obtain the final pglfA* construct.

The pΔglfA and pglfA* plasmids were linearized (KpnI/SacII) before polyethylene glycol-mediated fusion of protoplasts, as described previously (37). Transformants were grown on AMM plates containing 1.2 M sorbitol as the osmotic stabilizer under appropriate selection conditions and singled out twice before further analysis. Accurate gene deletion and reconstitution were confirmed by Southern hybridization. Southern probes were amplified from genomic DNA by using primer pairs PS66A/PS67A, PS68A/PS69A, and PS20/PS21. All primer sequences are provided in Table 1.

Western blot analysis. Cell wall glycoproteins and soluble polysaccharides were extracted from 30 mg ground *A. fumigatus* mycelium by incubation in 1 ml sample buffer (15% glycerol, 100 mM Tris-HCl, pH 6.8, 1.5% sodium dodecyl sulfate, 0.25% β-mercaptoethanol, 0.025% bromophenol blue) for 12 min at 95°C. A portion (20 μl) of the supernatant was separated on a 10% sodium dodecyl sulfate-polyacrylamide gel and transferred to nitrocellulose membranes. The monoclonal antibody (MAb) EB-A2 (42) conjugated to horseradish peroxidase (HRP) from a Platelia *Aspergillus* test (Bio-Rad, Hercules, CA) or HRP-coupled lectin concanavalin A (ConA) (Sigma-Aldrich) was used in a 1:50 dilution or at 0.2 μg/ml, respectively. HRP activity was visualized by an enhanced chemiluminescence system (Pierce, Rockford, IL).

N-glycan analysis. N-glycans of secreted glycoproteins in the supernatant of an *A. fumigatus* liquid culture were analyzed after peptide *N*-glycosidase F (PNGase F)-mediated release and 8-amino-1,3,6-pyrenetrisulfonic acid (APTS) labeling by capillary electrophoresis, as recently described (20). Separation was carried out on a four-capillary electrophoresis DNA sequencer (3130 genetic analyzer; Applied Biosystems, Foster City, CA). Oligomaltose and bovine RNase B N-glycans (Prozyme, San Leandro, CA) served as reference oligosaccharides.

Purification and analysis of GIPCs. Mycelia (0.5 g) ground in liquid nitrogen with a mortar and pestle were disrupted by sonication in 6 ml of $CHCl_3$-methanol (MeOH), 1:1. After addition of 3 ml $CHCl_3$ (to obtain a $CHCl_3$/MeOH ratio of 2:1), glycosylinositolphosphoceramides (GIPCs) were extracted at room temperature for at least 15 min on a rotating shaker. MeOH (3 ml) was then added to lower the density, and the mixture was centrifuged for 10 min at 2,000 × *g* to remove insoluble material. Chloroform and H_2O were then added to the supernatant to obtain a biphasic system with an 8:4:3 ratio of $CHCl_3$/MeOH/H_2O. After centrifugation for 10 min at 2,000 × *g*, GIPCs contained in the upper phase were collected and applied to a C_{18} SepPak cartridge (Waters, Eschborn, Germany) preequilibrated with 5 ml $CHCl_3$/MeOH/H_2O at a ratio of 3:48:47. After washing of the column with 20 ml $CHCl_3$/MeOH/H_2O at a ratio of 3:48:47, glycolipids were eluted with 5 ml MeOH and dried under a stream of nitrogen. High-performance thin-layer chromatography and immunostaining with the MAb MEST-1 were carried out as previously described (47).

Growth assay. For radial growth measurement, a 10-μl drop containing 10,000 *A. fumigatus* conidia was placed in the center of an agar plate containing either minimal (AMM) or complete (potato dextrose agar; Becton Dickinson Difco, Heidelberg, Germany) medium. Plates were incubated at various temperatures, and colony diameters were measured twice daily.

Antifungal susceptibility testing. The reference broth microdilution test was applied for *A. fumigatus* antifungal susceptibility testing (21). Each antifungal stock was diluted in 200 μl double-strength RPMI 2%G (RPMI 1640 liquid medium buffered with 165 mM 4-morpholinepropanesulfonic acid [MOPS] to

pH 7.0 and supplemented with 2% glucose) to obtain the highest concentration to be tested. Nine serial 1:2 dilutions in double-strength RPMI 2%G were made, and to each dilution a volume of 100 μl of an *A. fumigatus* spore solution ($2.5 \cdot 10^5$/ml in water) was added. Microtiter plates were incubated at 35°C, and fungal growth in each well was read out visually after 3 days and compared to growth in control wells that contained no antifungal.

Field emission scanning electron microscopy. For morphological studies and measurements of the cell wall thickness, *A. fumigatus* wt and Δ*glfA* mutant mycelia were fixed in 5% formaldehyde and 2% glutaraldehyde in cacodylate buffer (0.1 M cacodylate, 0.01 M $CaCl_2$, 0.01 M $MgCl_2$, 0.09 M sucrose, pH 6.9) for 1 h on ice. Samples were washed several times with cacodylate buffer and subsequently with TE buffer (20 mM Tris-HCl, 1 mM EDTA, pH 6.9) before dehydration in a graded series of acetone (10, 30, 50, 70, 90, and 100%) on ice for 15 min per step. Samples at the 100% acetone step were allowed to reach room temperature before another change in 100% acetone. Samples were then subjected to critical-point drying with liquid CO_2 (CPD 30; Balzers Union, Liechtenstein). Dried samples were then mounted onto conductive carbon adhesive tabs on an aluminum stub and sputter coated with a thin gold film (SCD 40; Balzers Union, Liechtenstein). For cell wall thickness measurements, mycelium was fractured by pressing another conductive carbon adhesive tab-covered stub onto the sample and separating both stubs immediately thereafter. Fractured hyphae were also made conductive by sputter coating with a gold film before examination with a field emission scanning electron microscope (Zeiss DSM 982 Gemini) using an Everhart Thornley SE detector and an in-lens SE detector at a 50:50 ratio at an acceleration voltage of 5 kV and at calibrated magnifications.

Mouse infection model. A low-dose mouse infection model of invasive aspergillosis for BALB/c mice which had been established previously (25) was essentially used. The immunosuppressive state was established by intraperitoneal injections of 100 mg cyclophosphamide (Endoxan; Baxter Chemicals)/kg of body weight on days −4, −1, 0, 2, 5, 8, and 11 and a single subcutaneous dose (200 mg/kg) of a cortisone acetate suspension (Sigma) on day −1. Groups of 20 mice were infected intranasally with 20,000 conidia of the wt strain, the Δ*glfA* strain, or the reconstituted *glfA** strain on day 0. The control group received phosphate-buffered saline (PBS) only. Survival was monitored for 13 days after infection, and moribund animals were sacrificed. Coincidence of severely reduced mobility, low body temperature, and breathing problems was defined as the moribundity criterion. Statistical analysis of survival data was carried out using a log rank test implemented in Prism 4 (GraphPad Software, San Diego, CA). For quantification experiments, groups of three to five animals were killed 2, 4, and 6 days after infection and lungs were removed for further analysis.

Lung histology. Female BALB/c mice were immunosuppressed and infected as described above. The animals were killed after 5 days and their lungs removed and fixed in 4% PBS-buffered paraformaldehyde overnight. Tissue samples were dehydrated through a series of graded alcohols, cleared with xylene, and embedded in paraffin. Tissue sections (5 μm) were stained either with hematoxylin/eosin or by the periodic acid-Schiff method for visualization of fungal cell walls. Photomicrographs were taken with an Axiovert 200M microscope (Zeiss, Germany) at ×10 and ×20 magnifications.

Preparation of genomic DNA from mouse lungs. Tissue homogenization was essentially as described previously (7). Immediately after removal, mouse lungs were transferred to a 2-ml screw cap containing 1.4-mm ceramic beads (lysing matrix D; Qbiogene, Irvine, CA) and 20% glycerol-PBS. Tissue was disrupted using a FastPrep FP120 instrument (Qbiogene) three times for 30 s each at speed 5, with intermediate cooling on ice. The disrupted tissues were further homogenized with approximately 250 mg acid-washed glass beads (0.45 to 0.5 mm; Sigma-Aldrich) by vortexing three times for 30 s each, with intermediate cooling on ice. A DNeasy blood and tissue kit (Qiagen, Hilden, Germany) was used to extract genomic DNA from an equivalent of 8% of the starting tissue material of this homogenate. DNA was finally recovered in 200 μl elution buffer.

qPCR. Quantitative PCR (qPCR) was carried out essentially as described previously (7). Primers for amplification of an 18S rRNA gene (GenBank accession number AB008401) fragment specific for *A. fumigatus* and a hybridization probe labeled with 6-carboxyfluorescein (FAM) (5′ end) and 6-carboxytetramethylrhodamine (3′ end) were designed using Primer Express software, version 3.0 (Applied Biosystems) (Table 1). qPCR reactions were performed with a 7500 Fast real-time PCR system instrument (Applied Biosystems) loaded with MicroAmp optical 96-well plates sealed with an optical adhesive cover (Applied Biosystems). Each qPCR reaction mixture (20 μl) contained 5 μl sample DNA, 250 nM dual-labeled hybridization probe, 500 nM primers, 250 μg/ml bovine serum albumin, and TaqMan Fast universal PCR master mix (Applied Biosystems). The latter contains hot-start DNA polymerase, deoxynucleoside triphosphates, and the fluorescent dye carboxyrhodamine (ROX) as a passive reference. Real-time PCR data were acquired using Sequence Detection software, v1.3.1. The FAM/ROX fluorescence ratio was recorded at every cycle, and a threshold cycle (C_T) value was assigned to each reaction product, defining the cycle number at which the FAM/ROX signal surpassed an automatically defined threshold. C_T values were corrected for differences in yield of genomic DNA by normalization to the DNA concentration of a control sample by using the formula $C_{T,\mathrm{norm}} = C_{T,\mathrm{measured}} + \log_2(\mathrm{DNA}_{\mathrm{sample}}/\mathrm{DNA}_{\mathrm{control}})$ (7). Translation of sample $C_{T,\mathrm{norm}}$ values into rRNA gene copy numbers was done as follows. C_T values of serial 1:10 dilutions containing 300 to 300,000 molecules (n) (calculated from M_w and DNA concentration determined by measurement of optical density at 260 nm) of a plasmid bearing the cloned *A. fumigatus* 18S rRNA gene were plotted against n to generate a calibration curve which was then used to assign an rRNA gene copy number to a given sample $C_{T,\mathrm{norm}}$ value. Conidial equivalents were calculated from gene copy numbers by means of uninfected tissue samples that were spiked with defined numbers of conidia before tissue homogenization (7). Samples, controls, and standards were analyzed in triplicate.

RESULTS

Deletion and reconstitution of the *glfA* gene in *A. fumigatus*. To begin investigating the role of Gal*f* in *A. fumigatus* biology, we deleted the gene encoding UGM (GenBank accession no. AJ871145) and named it *glfA*, following the recommendations for gene naming for *Aspergillus*. To do this, we generated a deletion plasmid containing the regions flanking the *glfA* coding sequence separated by the bifunctional selection cassette phleo/tk, which confers both resistance to phleomycin and sensitivity to FUDR (18). This construct was used to transform protoplasts of *A. fumigatus* clinical strain D141, which served as the wt, and phleomycin-resistant transformants were analyzed by Southern blotting using several digoxigenin-labeled probes (Fig. 1). One of the clones that had undergone the desired gene replacement (Fig. 1) was selected for further analysis and named Δ*glfA*.

The selected disruptant was further subjected to protoplast transformation with a large DNA fragment encompassing the *glfA* coding sequence which contained a single translationally silent nucleotide exchange that generated an XhoI restriction site. Gene replacement in the transformants resulted in the reconstitution of the *glfA* locus (Fig. 1) as detected by FUDR resistance and proven by Southern blot analysis for a selected clone named *glfA** (Fig. 1B). The silent mutation introduced in the reconstituted strain allowed differentiation between the wt and the *glfA** mutant, as demonstrated in Fig. 1B (top), and thus enabled us to rule out contamination by the wt strain. The reconstitution of the *glfA* locus ensures that any phenotype observed for the Δ*glfA* strain can be reverted and hence be securely attributed to the loss of the *glfA* gene.

Gal*f* is absent from the *A. fumigatus* Δ*glfA* mutant. To confirm that deletion of *glfA* indeed altered the expression of Gal*f*-containing glycoconjugates, aqueous mycelial extracts were tested for reactivity to the Gal*f*-specific MAb EB-A2. This antibody recognizes preferably β1,5-linked Gal*f* residues that are present in all forms of galactomannan (cell wall bound, membrane bound, and secreted) (42) as well as in some O-glycans (23). Moreover, a second binding epitope, Gal*f*(β1,2) Man, which is part of galactofuranosylated N-glycans, has been postulated (29). Thus, EB-A2 can be used to detect galactomannan and galactofuranosylated glycoproteins simultaneously. Western blot analysis of wt and *glfA** total mycelial extracts labeled with HRP-conjugated EB-A2 revealed a smear migrating around 40 to 80 kDa, in accordance with previous

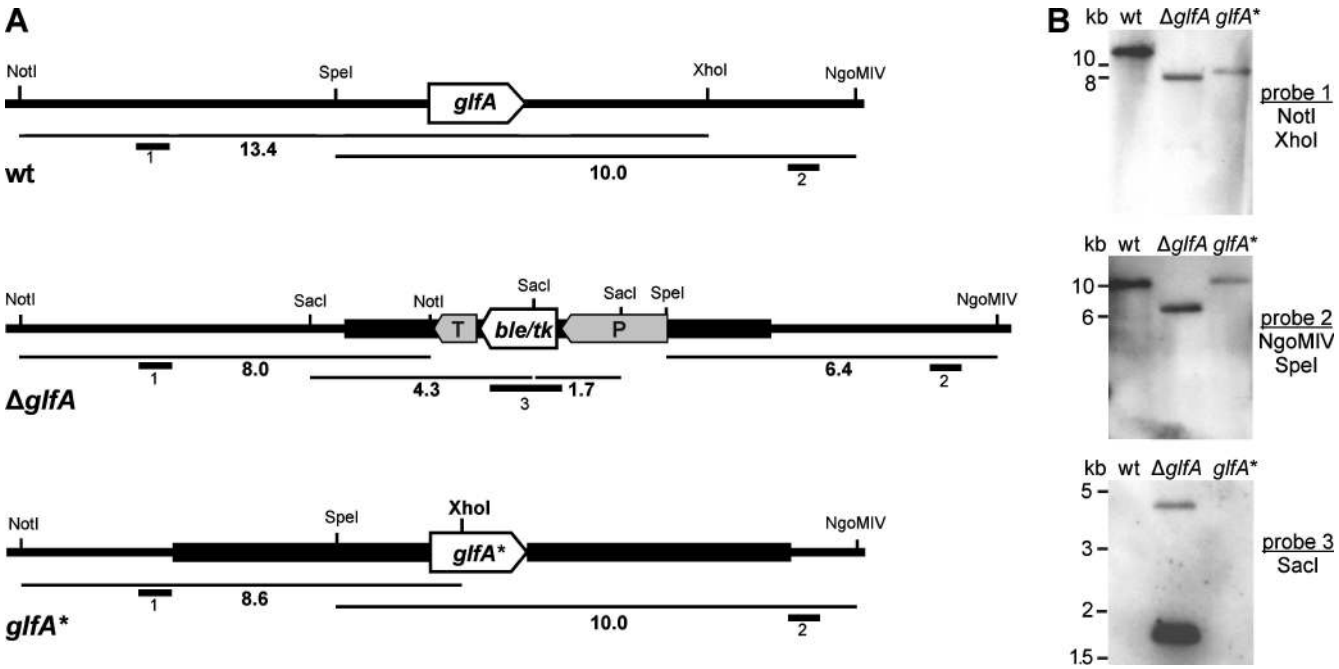

FIG. 1. (A) Schematic representation of the chromosomal *glfA* locus in wt, Δ*glfA*, and reconstituted *glfA** strains. The thick black bars show flanking regions used for homologous recombination. The positions of probes (probes 1 to 3) used for Southern blot analysis, along with the respective restriction fragments (sizes in kb), are indicated. *ble*/*tk*, phleomycin resistance/thymidine kinase fusion gene; P, promoter; T, terminator. (B) Southern blots of genomic DNA digested with the indicated restriction enzymes and hybridized to different digoxigenin-labeled probes.

findings (42). In contrast, the Δ*glfA* mycelial extract was not stained at all, indicating the absence of Gal*f* in the galactomannan and glycoproteins of this mutant (Fig. 2A, left). ConA used as the loading control bound slightly better to the Δ*glfA* extract than to those of the wt and the *glfA** mutant (Fig. 2A, right). The lack of Gal*f* in the Δ*glfA* mutant might increase the accessibility of the mannan for ConA and thus could explain this finding.

Similarly, the absence of Gal*f* in Δ*glfA* glycolipids was shown by the absence of reactivity to the MAb MEST-1. This antibody, which recognizes β1,3- and β1,6-linked Gal*f* residues (43), labeled several *A. fumigatus* GIPCs after separation by high-performance thin-layer chromatography, as previously shown (47), but did not label glycosphingolipids extracted from the Δ*glfA* mutant (Fig. 2B, left). The upper bands observed in Fig. 2B (left panel) might be attributed to GIPCs containing one or two Gal*f* and two or three mannose residues, as recently described (41, 47). In addition, Simenel et al. (41) reported an unusual GIPC containing a Gal*f* residue substituted at position 6 by a choline phosphate. The lower band present in the wt chromatogram could correspond to a similar GIPC. Staining of glycolipids by orcinol was used as the loading control (Fig. 2B, right). The simpler Δ*glfA* chromatogram is compatible with the absence of Gal*f*-containing GIPCs. The uppermost band observed in the chromatogram most probably corresponds to Man(α1,3)Man(α1,2)Ins-P-Cer, while the band just beneath it could be attributed to Man(α1,2)Man(α1,3)Man(α1,2)Ins-P-Cer (47). The chromatograms obtained from the reconstituted *glfA** mutant and the wt were indistinguishable (data not shown).

Additionally, N-glycans enzymatically released from *A. fu-*

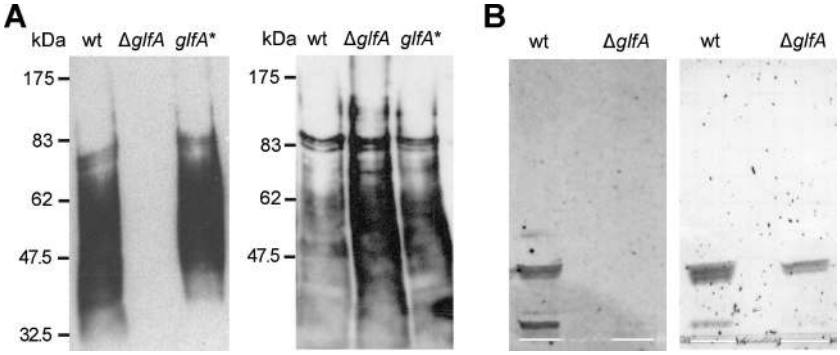

FIG. 2. (A) Western blots of *A. fumigatus* mycelial extracts containing glycoproteins and cell wall polysaccharides stained with HRP conjugates of either Gal*f*-specific MAb EB-A2 (left) or α-mannose binding lectin ConA (right). (B) *A. fumigatus* GIPCs separated by high-performance thin-layer chromatography and stained with Gal*f*-specific MAb MEST-1 (left) or orcinol (right). White bars indicate the origin.

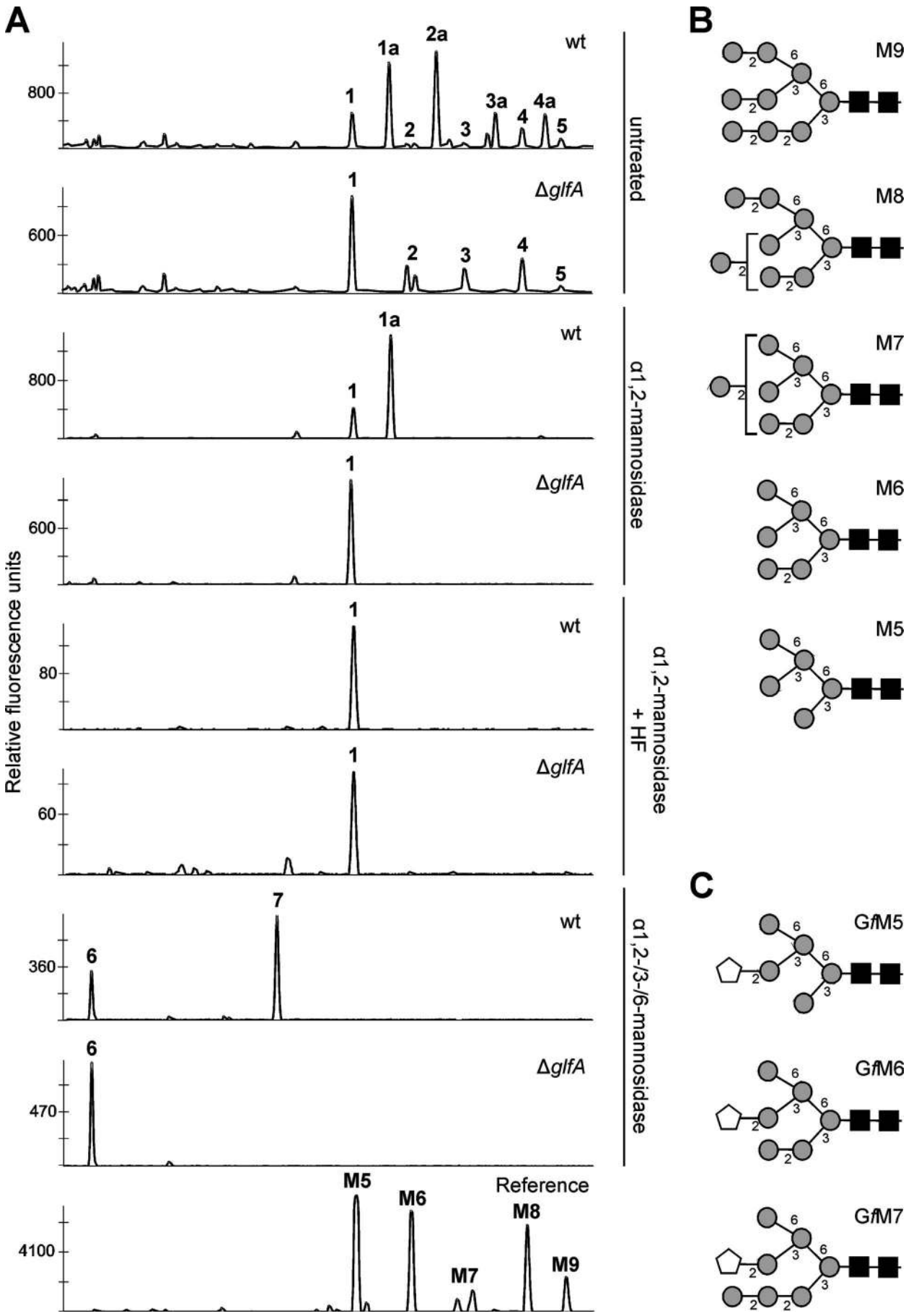

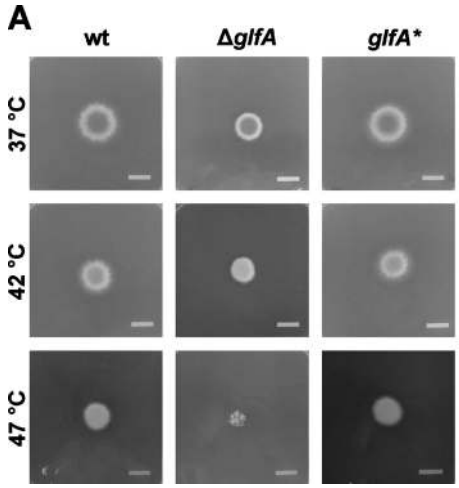

B

	Growth rate [µm/h]	rel.	P
37 °C			
wt	654	1	
Δ*glfA*	270	0.41	***
*glfA**	670	1.02	ns
42 °C			
wt	546	1	
Δ*glfA*	137	0.25	***
*glfA**	536	0.98	ns
47 °C			
wt	235	1	
Δ*glfA*	68	0.29	***
*glfA**	257	1.09	ns

FIG. 4. (A) Colony morphology of *A. fumigatus* on minimal agar after 2 days. Bar, 1 cm. (B) Absolute and relative (rel.) (compared to the wt) growth rates derived from three independent experiments. *P* values derived from a *t* test indicate statistical significance (***, $P < 0.001$; ns, not significant).

migatus secreted proteins were analyzed by capillary electrophoresis after fluorescent labeling (8, 20). The profiles obtained are presented in Fig. 3A (panels 1 and 2). The peaks labeled 1, 2, 3, 4, and 5 present in both electropherograms comigrated with reference oligosaccharides M5 to M9 (Fig. 3A, panel 9, and 3B). Moreover, digestion of these N-glycans by *Trichoderma reesei* α1,2-mannosidase indicates that peaks 2, 3, 4, and 5 arise from substitution of oligosaccharide 1 with one to four mannose residues linked in α1,2 (Fig. 3A, panels 3 and 4). The profile obtained with wt N-glycans (Fig. 3A, panel 1) presents four additional peaks (labeled 1a, 2a, 3a, and 4a) that were absent from *glfA* N-glycans. The retention times of these peaks suggest that they arise from substitution of oligosaccharides 1 to 4 with a single Gal*f* residue. The presence of a terminal nonreducing Gal*f* residue in *A. fumigatus* N-glycans has been reported previously (9) and was demonstrated by hydrofluoric acid treatment of the N-glycans after *T. reesei* α1,2-mannosidase digestion (Fig. 3A, panels 5 and 6). This mild acid treatment, known to release Gal*f*, entirely converted oligosaccharide 1a into oligosaccharide 1 (Fig. 3A, panels 3 and 5). In contrast, hydrofluoric acid treatment did not change the profile of Δ*glfA* N-glycans digested with α1,2-mannosidase (Fig. 3A, panels 4 and 6).

Interestingly, the comparison of wt and Δ*glfA* N-glycans digested with *T. reesei* α1,2-mannosidase or jack bean mannosidase helps with positioning of the Gal*f* residue. α1,2-Mannosidase treatment converted the oligosaccharides 2a, 3a, and 4a into 1a while the oligosaccharides 2, 3, and 4 generated 1 (Fig. 3A, compare panels 1 and 2 with panels 3 and 4). This indicates that the Gal*f* residue does not protect any mannose residues from the exomannosidase digestion and thus does not substitute an α1,2-linked mannose (Fig. 3A, panels 3 and 4). Moreover, jack bean mannosidase digestion of wt N-glycans resulted in a major peak (peak 7), attributed to Gal*f*$Man_3GlcNAc_2$ from its retention time, in addition to $Man_1GlcNAc_2$ (peak 6), expected from digestion of high-mannose type N-glycans (Fig. 3A, panels 7 and 8). These experiments do not allow for the determination of the detailed N-glycan structures but suggest that they resemble the N-glycans of *A. niger* α-glucosidase and α-galactosidase (44, 45). More importantly, these experiments demonstrate the absence of Gal*f* in the Δ*glfA* N-glycans.

Loss of Gal*f* alters morphology and growth of *A. fumigatus*. The Δ*glfA* strain exhibited a marked growth defect on solid minimal media or complete media compared to the wt. This effect could be observed for a wide range of temperatures (Fig. 4) and was statistically different in all cases ($P < 0.001$, *t* test, $n = 3$). The most severe effect was found at 42°C, with a 75% reduction in radial growth (Fig. 4B). In parallel, Δ*glfA* conidiation was diminished by 90% at 37°C and was almost absent at 42°C. In contrast, the onsets and rates of germination of wt, Δ*glfA*, and *glfA** conidia were similar. In minimal media at 37°C, the conidia of all strains started forming germ tubes at 3.2 h and reached 100% germination within 8 to 9 h (data not shown).

Scanning electron micrographs of intact mycelium, conidiophores, and conidia of Δ*glfA* did not reveal any obvious morphological differences when compared to wt. However, the observation of fractured mycelium revealed a marked reduction of the Δ*glfA* cell wall thickness (Fig. 5). Measurements indicated that the cell wall thickness of wt *A. fumigatus* varies from 85 to 315 nm, which is in good agreement with earlier findings (39). In contrast, Δ*glfA* cell wall thickness ranged from

FIG. 3. (A) Electropherograms of fluorescently labeled N-glycans enzymatically released from secreted *A. fumigatus* glycoproteins. Oligosaccharides from the wt and the Δ*glfA* mutant were untreated (panels 1 and 2), digested with *T. reesei* α1,2-exomannosidase with or without hydrofluoric acid (HF) treatment (panels 3 to 6), or digested with jack bean α-mannosidase (panels 7 and 8). Bovine RNase B N-glycans served as the reference (panel 9). (B) Structures of bovine RNase B reference N-glycans. (C) Major N-glycans found on *A. niger* α-galactosidase and α-glucosidase (44, 45). Black squares, *N*-acetylglucosamine; gray circles, mannose; white pentagon, galactofuranose.

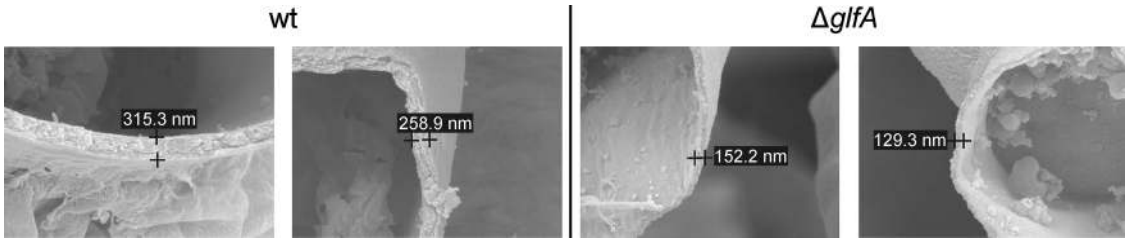

FIG. 5. Field emission scanning electron micrographs of cross-fractured mycelial walls of *A. fumigatus* wt and Δ*glfA* hyphae. Panels 1 and 3 display the highest measurement of cell wall thickness. Panels 2 and 4 present two measurements illustrating the 50% reduction of Δ*glfA* cell wall thickness.

85 to 150 nm. The mean values (±standard deviations) of cell wall thickness obtained from 25 measurements were 227.5 nm (±15.98 nm) and 109.7 nm (±11.3 nm) for wt and Δ*glfA* hyphae, respectively. The cell wall of Δ*glfA* was thus approximately half the thickness of the wt cell wall.

Δ*glfA* is more susceptible to drugs. The structural cell wall defect caused by the Gal*f* deficiency was accompanied by an increased susceptibility to several antifungal agents (Table 2). MICs determined by a broth microdilution test were slightly reduced for amphotericin B and caspofungin in the Δ*glfA* mutant. A more pronounced increase in susceptibility was seen for voriconazole (0.04 mg/liter for Δ*glfA*, compared to 0.3 mg/liter for the wt) and nikkomycin Z (63 to 125 mg/liter for Δ*glfA* and 500 mg/ml for the wt), suggesting an increased permeability of the cell wall caused by the loss of Gal*f*. In contrast, the sensitivity toward oxidative stress remained unchanged, as indicated by equal MICs for H_2O_2 in both wt and Δ*glfA* strains.

Δ*glfA* displays attenuated virulence in a murine model of invasive aspergillosis. The influence of the *glfA* deletion on the pathogenicity of *A. fumigatus* was assessed in a low-dose mouse infection model of invasive aspergillosis (25). Cyclophosphamide was used to induce neutropenia in female BALB/c mice, and a single dose of cortisone acetate was administered before intranasal infection with 20,000 *A. fumigatus* conidia. Neutropenia was maintained throughout the observation period of 13 days, and survival was recorded daily (Fig. 6A). Ninety percent of the animals infected with the wt did not survive beyond day 7 after infection, whereas half of the mice infected with Δ*glfA* were still alive on day 13. A log rank test of wt and Δ*glfA* survival data confirmed that the observed difference was statistically significant ($P = 0.0004$). The attenuation in virulence could clearly be attributed to the absence of *glfA*, since animals infected with the reconstituted *glfA** strain showed a survival pattern nearly identical to that of the wt (no significant difference by the log rank test, $P = 0.559$). A histological examination of lung tissue from mice infected with the wt, Δ*glfA*, and *glfA** strains 5 days after inoculation showed evident fungal growth surrounding bronchioles and tissue penetration (Fig. 7). For each strain, inflammatory cells were rarely observed at the sites of infection.

To correlate the delay in the onset and progression of mortality with a growth defect, the fungal burden in lungs of infected mice was determined by qPCR (Fig. 6B). Mice were treated and infected as described above. After 2, 4, and 6 days, animals were sacrificed and their lungs taken. DNA was isolated from homogenized lung tissue and fungal content determined by amplification of a part of *A. fumigatus* ribosomal DNA. As shown in Fig. 6B, growth of Δ*glfA* was restricted in vivo compared to that of the wt, which was in agreement with the slower growth observed in vitro.

TABLE 2. MICs of various antifungal agents against *A. fumigatus* mutants, obtained from a broth microdilution assay

Genotype	MIC (mg/liter)[a] of:				
	AmB	Vor	Cas	NiZ	H_2O_2
wt	3.9	0.3	62.5	500	218
Δ*glfA*	2.0	0.04	31.3	62.5–125	218
*glfA**	3.9	0.3	62.5	500	218

[a] Values for amphotericin B (AmB) and caspofungin (Cas) are MIC_{90} values, values for voriconazole (Vor) and nikkomycin Z (NiZ) are MIC_{50} values, and values for H_2O_2 are MIC_{100} values.

DISCUSSION

The essential role of the β1,3-glucan in cell wall organization and growth of several pathogenic fungi has been the basis for the development of the echinocandins (11). Likewise, inhibitors of chitin biosynthesis are currently being explored as new antifungal drugs since chitin is an important structural element of the fungal cell wall (6). In contrast, although galactomannan is a major component of the cell wall and the extracellular matrix, the role of galactomannan had not yet been investigated, since the enzymes involved in its biosynthesis are unknown. Recently, we and others characterized the UGM of various pathogenic eukaryotes, including *A. fumigatus* (2, 5). In prokaryotes, like in the protozoan *Leishmania*, this enzyme is the only route to the formation of UDP-Gal*f*, the donor substrate of galactofuranosyltransferases, and thus controls the biosynthesis of all Gal*f*-containing molecules. Likewise, *A. fumigatus* UGM was found to be essential for the biosynthesis of galactomannan as well as some glycosphingolipids and glycoproteins. Like in other organisms (16, 32), deletion of the *glfA* gene resulted in the complete absence of Gal*f*, as shown for instance by the absence of reactivity to the antibody EB-A2.

Besides demonstrating the lack of Gal*f* in the Δ*glfA* mutant, our analyses provide useful structural information for *A. fumigatus* N-glycans. Treatment of wt secreted proteins with PNGase F released galactofuranosylated high-mannose type N-glycans. The size of the oligosaccharides and the presence of a single Gal*f* residue are in agreement with previous studies of filamentous fungi (26, 29). Moreover, analysis of these oligo-

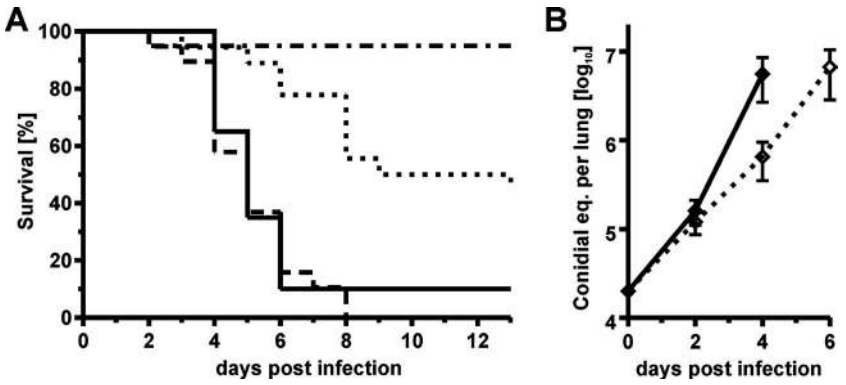

FIG. 6. (A) Survival of immunosuppressed mice infected intranasally with *A. fumigatus* wt (solid line), Δ*glfA* (dotted line), or *glfA** (dashed line) strains and of uninfected mice (dotted and dashed line). Each group consisted of 20 animals. (B) qPCR determination of *A. fumigatus* burden (measured as conidial equivalents [eq.] [see Materials and Methods]) in lung tissue from immunosuppressed mice infected with wt (solid line) or Δ*glfA* (dotted line) strains. Each data point represents the mean value obtained from three to five animals. Error bars indicate standard errors of the means.

saccharides after digestion by jack bean or *T. reesei* α1,2-mannosidase helps with positioning of the Gal*f* residue. These data and the comparison with high-mannose standards suggest that the N-glycans from *A. fumigatus* secreted proteins resemble those of *A. niger* α-D-galactosidase and α-D-glucosidase (44, 45, 49). These N-glycans might have arisen simply from trimming of the $Glc_3Man_9GlcNAc_2$ precursor and substitution by a Gal*f* residue. *Aspergillus* spp. indeed contain several α1,2-mannosidase genes, and trimming of high-mannose glycans has been shown previously (13, 52). Interestingly, Gal*f* addition has been suggested to act as a stop signal for mannose addition, in analogy to the role proposed for the α1,3-linked terminal mannose in *Saccharomyces cerevisiae* (29, 49). However, preventing the addition of galactofuranose does not result in an increased size of the oligosaccharides. On the contrary, $Man_5GlcNAc_2$ is the main oligosaccharide found in the Δ*glfA* mutant, while $Galf Man_6GlcNAc_2$ is predominant in the wt.

Although *glfA* deletion has been shown to be lethal in *Mycobacterium smegmatis* (32), the in vitro viability of the *A. fumigatus* Δ*glfA* mutant is unsurprising, since Gal*f* occupies a nonreducing terminal position in the molecules of this fungus. Hence, the absence of Gal*f* does not perturb the basic organization of the cell wall, as would the absence of the underlying structures. Nevertheless, it resulted in marked alterations of the cell surface and a notably thinner cell wall, as revealed by electron microscopy. The basis of this drastic change is unclear and difficult to attribute to a particular cell wall component, since glycosylphosphatidylinositol/cell wall bound galactoman-

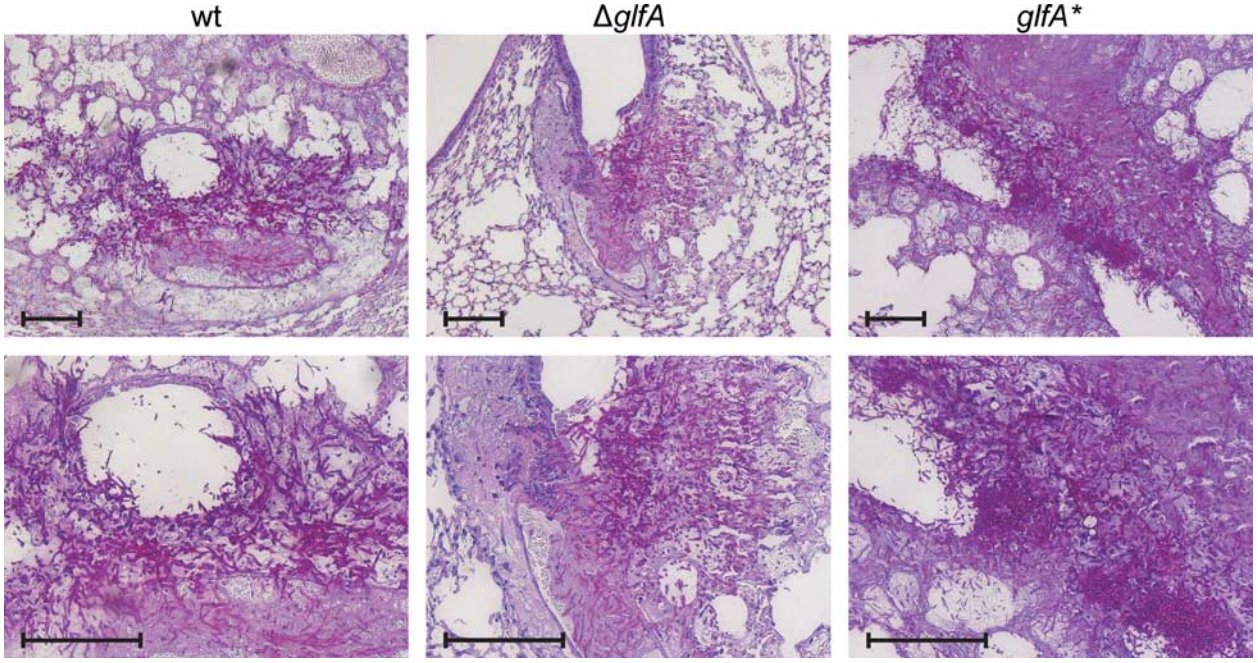

FIG. 7. Periodic acid-Schiff-stained lung sections of mice infected with wt, Δ*glfA*, or *glfA* A. fumigatus* strains. Fungal colonies appear purple/red. Infected sites are typically surrounded by areas of necrotic tissue but show no or hardly any infiltrating leukocytes. Bar, 100 μm.

nan, N-glycans, O-glycans, and GIPCs are affected by UDP-Gal*f* deficiency. In other fungi, the loss of terminal sugar residues has sometimes been associated with reduced cell wall strength. For instance, a *Schizosaccharomyces pombe* mutant deficient in cell wall galactosylation displays morphological changes, attenuated growth, and a 25 to 35% reduction in cell wall thickness (46).

The structural changes originating from the *glfA* deletion are associated with slower growth, indicating that Gal*f* plays an important role in *A. fumigatus* morphogenesis. The temperature-sensitive growth defect at a higher temperature displayed by the Δ*glfA* mutant is reminiscent of that observed for the ΔAf*Pmt1* mutant, a mutant characterized by reduced O glycosylation (53). Interestingly, an influence of Gal*f* deficiency on the growth rate was also observed for Δ*glfA* mutants of *Aspergillus nidulans* (F. H. Routier, unpublished data) and *Aspergillus niger* (10). Conversely, *glfA* deletion had no effect on the in vitro growth of *Leishmania* parasites (16), highlighting that the role of Gal*f* cannot be translated to every Gal*f*-containing organism.

The ability to thrive at 37°C is a characteristic of human pathogens that has been shown to correlate with virulence potential in the case of *A. fumigatus* (31). Consequently, mutations that affect the growth of fungi at mammalian body temperature are commonly associated with attenuated virulence (40). In this study, we observed slower growth of the *A. fumigatus* Δ*glfA* mutant in vitro but also in vivo by using qPCR. In agreement with this observation, the mutant was clearly attenuated in virulence, showing a delay in both the onset and the progression of mortality when tested in a low-dose mouse infection model of invasive aspergillosis. An altered immune response caused by the different cell wall structure of the Δ*glfA* mutant may also contribute to the attenuation in virulence. However, no differences in adherence and uptake of wt and Δ*glfA* conidia by murine bone marrow-derived dendritic cells or in production of tumor necrosis factor alpha or interleukin-10 by infected murine bone-marrow derived macrophages were observed (K. Kotz, F. Ebel, and F. H. Routier, unpublished data).

The value of echinocandins in invasive aspergillosis treatment resides in their synergistic effects with azoles and amphotericin B. Similarly, chitin synthesis inhibitors demonstrate synergy with echinocandins and azoles (24). These synergistic effects that offer new options for combination antifungal therapy are most likely due to greater cell wall permeability. We did note an increase in susceptibility of the Δ*glfA* mutant to several antifungal agents, notably to voriconazole. However, in the liquid culture conditions classically used for antifungal susceptibility testing, the fungus is not surrounded by an extracellular matrix. This extracellular matrix that delays the penetration of drug is rich in galactomannan (3) and is probably altered in the Δ*glfA* mutant, as suggested by the compact appearance of colonies on agar plates. In vivo, a greater increase in susceptibility of the Δ*glfA* mutant to drugs would therefore be expected. Besides the attenuated virulence, this suggests that inhibitors of UGM might be useful in antifungal therapy. The absence of Gal*f* biosynthesis in mammals would represent a considerable advantage for the development of antifungal drugs with selective toxicity.

ACKNOWLEDGMENTS

We thank Florian Länger, Frank Ebel, and Jakob Engel for their help with histopathology, cytokine analysis, and glycolipid analysis, respectively. Monika Berger, Verena Grosse, Sabine Schild, Olaf Macke, and Brigitte Philippens are thanked for excellent technical assistance, and Anita Straus and Helio Takahashi are thanked for the generous gift of the MEST-1 MAb. We are indebted to Rita Gerardy-Schahn for her constant support.

REFERENCES

1. **Aquino, V. R., L. Z. Goldani, and A. C. Pasqualotto.** 2007. Update on the contribution of galactomannan for the diagnosis of invasive aspergillosis. Mycopathologia **163:**191–202.
2. **Bakker, H., B. Kleczka, R. Gerardy-Schahn, and F. H. Routier.** 2005. Identification and partial characterization of two eukaryotic UDP-galactopyranose mutases. Biol. Chem. **386:**657–661.
3. **Beauvais, A., C. Schmidt, S. Guadagnini, P. Roux, E. Perret, C. Henry, S. Paris, A. Mallet, M. C. Prévost, and J. P. Latgé.** 2007. An extracellular matrix glues together the aerial-grown hyphae of *Aspergillus fumigatus*. Cell. Microbiol. **9:**1588–1600.
4. **Bernard, M., and J. P. Latgé.** 2001. *Aspergillus fumigatus* cell wall: composition and biosynthesis. Med. Mycol. **39**(Suppl 1)**:**9–17.
5. **Beverley, S. M., K. L. Owens, M. Showalter, C. L. Griffith, T. L. Doering, V. C. Jones, and M. R. McNeil.** 2005. Eukaryotic UDP-galactopyranose mutase (*GLF* gene) in microbial and metazoal pathogens. Eukaryot. Cell **4:**1147–1154.
6. **Borgia, P. T., and C. L. Dodge.** 1992. Characterization of *Aspergillus nidulans* mutants deficient in cell wall chitin or glucan. J. Bacteriol. **174:**377–383.
7. **Bowman, J. C., G. K. Abruzzo, J. W. Anderson, A. M. Flattery, C. J. Gill, V. B. Pikounis, D. M. Schmatz, P. A. Liberator, and C. M. Douglas.** 2001. Quantitative PCR assay to measure *Aspergillus fumigatus* burden in a murine model of disseminated aspergillosis: demonstration of efficacy of caspofungin acetate. Antimicrob. Agents Chemother. **45:**3474–3481.
8. **Callewaert, N., S. Geysens, F. Molemans, and R. Contreras.** 2001. Ultrasensitive profiling and sequencing of N-linked oligosaccharides using standard DNA-sequencing equipment. Glycobiology **11:**275–281.
9. **Costachel, C., B. Coddeville, J. P. Latgé, and T. Fontaine.** 2005. Glycosylphosphatidylinositol-anchored fungal polysaccharide in *Aspergillus fumigatus*. J. Biol. Chem. **280:**39835–39842.
10. **Damveld, R. A., A. Franken, M. Arentshorst, P. J. Punt, F. M. Klis, C. A. van den Hondel, and A. F. Ram.** 2008. A novel screening method for cell wall mutants in Aspergillus niger identifies UDP-galactopyranose mutase as an important protein in fungal cell wall biosynthesis. Genetics **178:**873–881.
11. **Denning, D. W.** 2002. Echinocandins: a new class of antifungal. J. Antimicrob. Chemother. **49:**889–891.
12. **Denning, D. W.** 2003. Echinocandin antifungal drugs. Lancet **362:**1142–1151.
13. **Eades, C. J., and W. E. Hintz.** 2000. Characterization of the class I alpha-mannosidase gene family in the filamentous fungus *Aspergillus nidulans*. Gene **255:**25–34.
14. **Fontaine, T., C. Simenel, G. Dubreucq, O. Adam, M. Delepierre, J. Lemoine, C. E. Vorgias, M. Diaquin, and J. P. Latgé.** 2000. Molecular organization of the alkali-insoluble fraction of *Aspergillus fumigatus* cell wall. J. Biol. Chem. **275:**27594–27607.
15. **Guan, S., A. J. Clarke, and C. Whitfield.** 2001. Functional analysis of the galactosyltransferases required for biosynthesis of D-galactan I, a component of the lipopolysaccharide O1 antigen of *Klebsiella pneumoniae*. J. Bacteriol. **183:**3318–3327.
16. **Kleczka, B., A. C. Lamerz, G. van Zandbergen, A. Wenzel, R. Gerardy-Schahn, M. Wiese, and F. H. Routier.** 2007. Targeted gene deletion of *Leishmania major* UDP-galactopyranose mutase leads to attenuated virulence. J. Biol. Chem. **282:**10498–10505.
17. **Köplin, R., J. R. Brisson, and C. Whitfield.** 1997. UDP-galactofuranose precursor required for formation of the lipopolysaccharide O antigen of *Klebsiella pneumoniae* serotype O1 is synthesized by the product of the $rfbD_{KPO1}$ gene. J. Biol. Chem. **272:**4121–4128.
18. **Krappmann, S., O. Bayram, and G. H. Braus.** 2005. Deletion and allelic exchange of the *Aspergillus fumigatus veA* locus via a novel recyclable marker module. Eukaryot. Cell **4:**1298–1307.
19. **Kremer, L., L. G. Dover, C. Morehouse, P. Hitchin, M. Everett, H. R. Morris, A. Dell, P. J. Brennan, M. R. McNeil, C. Flaherty, K. Duncan, and G. S. Besra.** 2001. Galactan biosynthesis in *Mycobacterium tuberculosis*. Identification of a bifunctional UDP-galactofuranosyltransferase. J. Biol. Chem. **276:**26430–26440.
20. **Laroy, W., R. Contreras, and N. Callewaert.** 2006. Glycome mapping on DNA sequencing equipment. Nat. Protoc. **1:**397–405.
21. **Lass-Flörl, C., M. Cuenca-Estrella, D. W. Denning, and J. L. Rodriguez-Tudela.** 2006. Antifungal susceptibility testing in *Aspergillus* spp. according to EUCAST methodology. Med. Mycol. **44:**319–325.
22. **Latgé, J. P., H. Kobayashi, J. P. Debeaupuis, M. Diaquin, J. Sarfati, J. M. Wieruszeski, E. Parra, J. P. Bouchara, and B. Fournet.** 1994. Chemical and

immunological characterization of the extracellular galactomannan of *Aspergillus fumigatus*. Infect. Immun. **62:**5424–5433.
23. **Leitão, E. A., V. C. Bittencourt, R. M. Haido, A. P. Valente, J. Peter-Katalinic, M. Letzel, L. M. de Souza, and E. Barreto-Bergter.** 2003. Beta-galactofuranose-containing O-linked oligosaccharides present in the cell wall peptidogalactomannan of *Aspergillus fumigatus* contain immunodominant epitopes. Glycobiology **13:**681–692.
24. **Li, R. K., and M. G. Rinaldi.** 1999. In vitro antifungal activity of nikkomycin Z in combination with fluconazole or itraconazole. Antimicrob. Agents Chemother. **43:**1401–1405.
25. **Liebmann, B., T. W. Mühleisen, M. Müller, M. Hecht, G. Weidner, A. Braun, M. Brock, and A. A. Brakhage.** 2004. Deletion of the *Aspergillus fumigatus* lysine biosynthesis gene *lysF* encoding homoaconitase leads to attenuated virulence in a low-dose mouse infection model of invasive aspergillosis. Arch. Microbiol. **181:**378–383.
26. **Maras, M., I. van Die, R. Contreras, and C. A. van den Hondel.** 1999. Filamentous fungi as production organisms for glycoproteins of bio-medical interest. Glycoconj. J. **16:**99–107.
27. **Mikusová, K., M. Belánová, J. Korduláková, K. Honda, M. R. McNeil, S. Mahapatra, D. C. Crick, and P. J. Brennan.** 2006. Identification of a novel galactosyl transferase involved in biosynthesis of the mycobacterial cell wall. J. Bacteriol. **188:**6592–6598.
28. **Mohr, J., M. Johnson, T. Cooper, J. S. Lewis, and L. Ostrosky-Zeichner.** 2008. Current options in antifungal pharmacotherapy. Pharmacotherapy **28:**614–645.
29. **Morelle, W., M. Bernard, J. P. Debeaupuis, M. Buitrago, M. Tabouret, and J. P. Latgé.** 2005. Galactomannoproteins of *Aspergillus fumigatus*. Eukaryot. Cell **4:**1308–1316.
30. **Nassau, P. M., S. L. Martin, R. E. Brown, A. Weston, D. Monsey, M. R. McNeil, and K. Duncan.** 1996. Galactofuranose biosynthesis in *Escherichia coli* K-12: identification and cloning of UDP-galactopyranose mutase. J. Bacteriol. **178:**1047–1052.
31. **Paisley, D., G. D. Robson, and D. W. Denning.** 2005. Correlation between *in vitro* growth rate and *in vivo* virulence in *Aspergillus fumigatus*. Med. Mycol. **43:**397–401.
32. **Pan, F., M. Jackson, Y. Ma, and M. McNeil.** 2001. Cell wall core galactofuran synthesis is essential for growth of mycobacteria. J. Bacteriol. **183:**3991–3998.
33. **Patterson, T. F.** 2006. Treatment of invasive aspergillosis: polyenes, echinocandins, or azoles? Med. Mycol. **44(**Suppl 1**):**357–362.
34. **Pedersen, L. L., and S. J. Turco.** 2003. Galactofuranose metabolism: a potential target for antimicrobial chemotherapy. Cell. Mol. Life Sci. **60:**259–266.
35. **Perea, S., G. Gonzalez, A. W. Fothergill, W. R. Kirkpatrick, M. G. Rinaldi, and T. F. Patterson.** 2002. In vitro interaction of caspofungin acetate with voriconazole against clinical isolates of *Aspergillus* spp. Antimicrob. Agents Chemother. **46:**3039–3041.
36. **Pontecorvo, G., J. A. Roper, L. M. Hemmons, K. D. MacDonald, and A. W. Bufton.** 1953. The genetics of *Aspergillus nidulans*. Adv. Genet. **5:**141–238.
37. **Punt, P. J., and C. A. van den Hondel.** 1992. Transformation of filamentous fungi based on hygromycin B and phleomycin resistance markers. Methods Enzymol. **216:**447–457.
38. **Reichard, U., S. Büttner, H. Eiffert, F. Staib, and R. Rüchel.** 1990. Purification and characterisation of an extracellular serine proteinase from *Aspergillus fumigatus* and its detection in tissue. J. Med. Microbiol. **33:**243–251.
39. **Reijula, K. E.** 1991. Two common fungi associated with farmer's lung: fine structure of *Aspergillus fumigatus* and *Aspergillus umbrosus*. Mycopathologia **113:**143–149.
40. **Rementeria, A., N. López-Molina, A. Ludwig, A. B. Vivanco, J. Bikandi, J. Pontón, and J. Garaizar.** 2005. Genes and molecules involved in *Aspergillus fumigatus* virulence. Rev. Iberoam. Micol. **22:**1–23.
41. **Simenel, C., B. Coddeville, M. Delepierre, J. P. Latgé, and T. Fontaine.** 2008. Glycosylinositolphosphoceramides in *Aspergillus fumigatus*. Glycobiology **18:**84–96.
42. **Stynen, D., J. Sarfati, A. Goris, M. C. Prévost, M. Lesourd, H. Kamphuis, V. Darras, and J. P. Latgé.** 1992. Rat monoclonal antibodies against *Aspergillus* galactomannan. Infect. Immun. **60:**2237–2245.
43. **Suzuki, E., M. S. Toledo, H. K. Takahashi, and A. H. Straus.** 1997. A monoclonal antibody directed to terminal residue of beta-galactofuranose of a glycolipid antigen isolated from *Paracoccidioides brasiliensis*: cross-reactivity with *Leishmania major* and *Trypanosoma cruzi*. Glycobiology **7:**463–468.
44. **Takayanagi, T., A. Kimura, S. Chiba, and K. Ajisaka.** 1994. Novel structures of N-linked high-mannose type oligosaccharides containing alpha-D-galactofuranosyl linkages in *Aspergillus niger* alpha-D-glucosidase. Carbohydr. Res. **256:**149–158.
45. **Takayanagi, T., K. Kushida, K. Idonuma, and K. Ajisaka.** 1992. Novel N-linked oligo-mannose type oligosaccharides containing an alpha-D-galactofuranosyl linkage found in alpha-D-galactosidase from *Aspergillus niger*. Glycoconj. J. **9:**229–234.
46. **Tanaka, N., M. Konomi, M. Osumi, and K. Takegawa.** 2001. Characterization of a *Schizosaccharomyces pombe* mutant deficient in UDP-galactose transport activity. Yeast **18:**903–914.
47. **Toledo, M. S., S. B. Levery, B. Bennion, L. L. Guimaraes, S. A. Castle, R. Lindsey, M. Momany, C. Park, A. H. Straus, and H. K. Takahashi.** 2007. Analysis of glycosylinositol phosphorylceramides expressed by the opportunistic mycopathogen *Aspergillus fumigatus*. J. Lipid Res. **48:**1801–1824.
48. **Trejo, A. G., J. W. Haddock, G. J. Chittenden, and J. Baddiley.** 1971. The biosynthesis of galactofuranosyl residues in galactocarolose. Biochem. J. **122:**49–57.
49. **Wallis, G. L., R. L. Easton, K. Jolly, F. W. Hemming, and J. F. Peberdy.** 2001. Galactofuranoic-oligomannose N-linked glycans of alpha-galactosidase A from *Aspergillus niger*. Eur. J. Biochem. **268:**4134–4143.
50. **Weston, A., R. J. Stern, R. E. Lee, P. M. Nassau, D. Monsey, S. L. Martin, M. S. Scherman, G. S. Besra, K. Duncan, and M. R. McNeil.** 1997. Biosynthetic origin of mycobacterial cell wall galactofuranosyl residues. Tuber. Lung Dis. **78:**123–131.
51. **Wing, C., J. C. Errey, B. Mukhopadhyay, J. S. Blanchard, and R. A. Field.** 2006. Expression and initial characterization of WbbI, a putative D-Gal*f*: alpha-D-Glc beta-1,6-galactofuranosyltransferase from *Escherichia coli* K-12. Org. Biomol. Chem. **4:**3945–3950.
52. **Yoshida, T., Y. Kato, Y. Asada, and T. Nakajima.** 2000. Filamentous fungus *Aspergillus oryzae* has two types of alpha-1,2-mannosidases, one of which is a microsomal enzyme that removes a single mannose residue from Man9GlcNAc2. Glycoconj. J. **17:**745–748.
53. **Zhuo, H., H. Hu, L. Zhang, R. Li, H. Ouyang, J. Ming, and C. Jin.** 2007. *O*-Mannosyltransferase 1 in *Aspergillus fumigatus* (AfPmt1p) is crucial for cell wall integrity and conidium morphology, especially at an elevated temperature. Eukaryot. Cell **6:**2260–2268.